Spectral, Thermal and Microbial Studies of a Transition Metal-Based Coordination Polymer Derived from a Terpolymer (Resorcinol, Formaldehyde, Urea) Ligand

Abdulrahman Mohammad[1], Abdul Kareem[1], Azar Ullah Mirza[1], Shahnawaz Ahmad Bhat[1], Paramjit Singh[1], Sahab A. A. Nami[2], Sultan A Nasar[3], Rilwanu Yahaya Kwanga[4] and Nahid Nishat[1]*

[1]Inorganic Materials Research Laboratory, Department of Chemistry, Jamia Millia Islamia, Delhi India.
[2]Department of Kulliyat, Faculty of Unani Medicine, Aligarh Muslim University, Aligarh India
[3]Department of Polymer Science, University of Madras, Chennai India
[4]Department of Microbiology, Kebbi State University of Science & Technology, Aliero Nigeria
*Corresponding author (e-mail: nishat_nchem08@yahoo.com)

A terpolymer resin derived from resorcinol, formaldehyde and urea (RFU) was synthesized through a condensation reaction. The transition metal ions of Mn(II), Co(II), Ni(II), Cu(II) and Zn(II) acetates were incorporated into the resin, yielding polymer-metal complexes. Gel permeation chromatography (GPC) was employed to determine the molecular weight of the terpolymer resin, while FTIR, UV-Vis, XRD, ^{1}H NMR, TGA, SEM and EDX analyses were conducted on the resin and its complexes. Thermal analysis revealed that the metal complexes were more stable compared to the terpolymer ligand, while EDX studies confirmed the binding of the metals to the ligand. The antibacterial activity of the synthesized materials was investigated against six strains of Gram-positive bacteria (S. *aureus, S. mutans, S. pyrogenes, S. epidermidis, B. cereus,* and *C. xerosis*) and four strains of Gram-negative bacteria (*E. coli, K. pneuomonieae, P. aeruginosa,* and *P. vulgaris*). It showed that all the materials were sensitive towards the tested organisms, with RFU-Co(II) having the most promising results. Antifungal activity tests against *A. niger, C. albicans, P. notatum,* and *S. cerevisiae* revealed that all the materials were insensitive towards these organisms.

Keywords: Terpolymer; ligand; coordination polymer; metal complex; antibacterial activity

Received: November 2023; Accepted: April 2024

Resorcinol is an isomer of benzenediol which plays a vital role in the synthesis of resins [1-2] and also in the synthesis of pharmaceutical materials [3-4] and other organic compounds [4-5]. Indeed, the compound plays an important role in ketose determination [6-7], and in the formation of thermoset resin when reacted with formaldehyde [8]. On the other hand, the amide compound urea (which possesses two NH_2 groups bonded to the carbonyl group) is of paramount importance in coordination chemistry [9], and in the biology of nitrogen containing materials [10]. Perhaps the aforementioned properties have made resorcinol and urea suitable for certain types of chemical reactions [11-13] like polymer formation, base-catalysed reactions, and construction of supramolecular compounds. Thus, in the presence of a binder like formaldehyde, a polymer can be formed with these or similar compounds [14-15]. The reaction of resorcinol and urea in the presence of formaldehyde leads to the availability of two hydroxyl groups and two NH groups, which makes it feasible for the chemistry of O and N donor ligands [16]. Research into the use of O and N donor ligands with transition metals has seen a surge in the last decade, especially in the medical and pharmaceutical fields [17-18].

In this work, we report the synthesis of a terpolymer (RFU) ligand derived from resorcinol, formaldehyde and urea through a condensation reaction, and the subsequent formation of coordination polymers with the transition metal ions Mn(II), Co(II), Ni(II), Cu(II), and Zn(II). The ligand and its metal polychelates were tested for their antibacterial and antifungal activities.

EXPERIMENTAL

Materials

The reagents used were resorcinol (Thomas Baker Chemicals, 99.0%), formaldehyde (Merck, 37%), urea (Merck, 99.5%), manganese (II) acetate 4-hydrate (Merck, 99.5%), cobaltous acetate (Fisher, 99%), nickel acetate tetrahydrate (Fine-Chem, 96%), copper (II) acetate monohydrate (Merck, 98%), and zinc acetate (Fine-Chem, 98.5%). All chemicals and metal salts were used without further purification.

Instrumentation

Ultraviolet visible spectroscopy (UV-Vis) spectra of the materials were recorded using a V3900 Hitachi spectrometer at room temperature in the range of 200-700 nm, with DMSO solvent and a scan rate of 600 nm/min. Fourier Transform infrared spectroscopy (FT-IR) spectra of the samples were recorded on a Bruker Tensor-37 spectrometer with the use of KBr pellets in the range of 4000-400 cm^{-1}. The X-ray diffraction (XRD) spectra of the materials were recorded using a Rigaku Ultima IV X-ray diffractometer with diffraction intensities ranging from 10-80° 2-Theta, and a scan rate of 10 min^{-1}. Proton nuclear magnetic resonance (^{1}H NMR) spectra were recorded on a 400 MHZ Bruker Avance-II NMR using DMSO solvent and tetramethyl silane (TMS) as a reference. Scanning electron microscopy (SEM) was conducted using a Zeiss V5.05 instrument at the voltage rate of 20 kV. Energy dispersive spectra (EDS) of the materials were recorded using a Rigaku instrument (a facility attached to the SEM). Thermogravimetric analysis (TGA) of the materials was conducted with a Mettler Toledo TGA/DSC, under a nitrogen atmosphere with a heating rate of 10k/min^{-1}.

Microbial Studies

Antibacterial assessment of the RFU terpolymer ligand and its metal polychelates were conducted according to a previously reported procedure [19]. The anti-bacterial activity of the compounds, namely RFU, RFU-Mn(II), RFU-Co(II), RFU-Ni(II), RFU-Cu(II) and RFU-Zn(II), were determined with the use of Ciprofloxacin (for Gram-positive strains), and Gentamicin (for Gram-negative strains) via the agar well diffusion method against Gram-positive (*Staphylococcus aureus, Streptococcus mutans, Streptococcus pyrogenes, Staphylococcus epidermidis, Bacillus cereus* and *Corynebacterium xerosis*), and Gram-negative (*Escherichia coli, Klebsiella pneumonia, Pseudomonas aeruginosa* and *Proteus vulgaris*) species. Nutrient agar No. 2 was applied in solid media for the preparation of nutrient plates, and nutrient broth was used for the preparation of plates in liquid media. The cultures were adjusted to 0.5 Farland standard and then agar media of 20 ml was poured into each Petri dish and kept for 15 min for adsorption to take place. The wells were placed into the seeded agar plates which were loaded with 100 µl of the test sample reconstituted in dimethyl sulphoxide (DMSO). Incubation of plates was carried out at 37 °C for 24 hours, and the antibacterial activity of the synthesized materials was tested by measuring the zone of growth inhibition against the test organism using an antibiotic zone scale. A medium containing DMSO as solvent was used as the negative control, whereas media containing Ciprofloxacin (5 µg/disc) and Gentamicin (10 µg/disc) were used as positive controls. The procedure was performed in triplicate.

Antifungal studies of the synthesized compounds were performed with the well diffusion method using casitone agar, and the organisms selected were *Aspergillus niger, Candida albicans, Penicillium notatum* and *Saccharomyces cerevisiae*. The inoculum used was prepared using fungal strains freshly sub-cultured on sterile sabouraud dextrose agar and incubated at 30 °C for 3-7 days. The resultant cells and spores were washed into sterile normal saline solution (0.85 %). The turbidity of the suspension was adjusted to match the 0.5 Farland standard, and 20 ml of Bacto-casitone was melted, cooled at 55 °C and then inoculated with 1 ml of the organism suspension. The inoculated agar was poured into the sterile plate (9 cm in diameter), and allowed to cool down on a level surface. Once the medium had solidified, four wells, each 4 mm in diameter, were cut out of the agar using a cock borer, and 20 µl of the synthesized compounds were placed into each well. The plate was incubated at 30 °C for 24 hours and the zone of inhibition was measured using a ruler.

Synthesis of the Terpolymer Ligand

The terpolymer (RFU) ligand was prepared according to a previously reported method [20] through the condensation reaction of resorcinol, formaldehyde and urea. Resorcinol solution (10 g) was placed in a 250 ml round bottom flask and dissolved in 15 ml DMF. A solution of urea (6 g) was placed in a 100 ml beaker and dissolved in 10 ml DMF. Both solutions were mixed in the 250 ml flask and formaldehyde (7.5 ml) was added dropwise to the mixture. A few drops of 2M HCl was also added to the mixture which was then placed in an oil bath and refluxed for 5 hours at 80°C with constant stirring. A reddish product (resin) was obtained after the reflux, which was then washed with hot water to remove the unreacted monomers. Purification of the resin was carried out by dissolution in 8 % NaOH and reprecipitation through the dropwise addition of 1:1 (vol/vol) HCl/water with constant stirring. The product was filtered off and washed with hot water to remove chloride ions. The purified RFU terpolymer was ground and kept in a vacuum over silica gel. The percentage yield of the RFU resin was found to be 69-74 %.

IR (film): 3515 cm^{-1}, 3437 cm^{-1}, 3417 cm^{-1} (υ N-H stretching), 3226 cm^{-1} (υ O-H stretching), 2995 cm^{-1} (υ C-H stretching), 1407 cm^{-1}, 1139 cm^{-1} (methylene bridge), 1321 cm^{-1} (in-plane bending δ OH), 1640 cm^{-1} (N-H bending), 1202 cm^{-1}, 971 cm^{-1} (sub. aromatic rings), 1502 cm^{-1} (υ C=O stretching). UV-Vis. 285 nm br., 540 nm w. ^{1}H NMR (400 MHZ DMSO-d_6) δ [ppm]: 2.72, 2.88 ($2CH_3$, s), 4.03, 4.26 ($2CH_2$, s), 5.41, 5.7 (4OH, m), 6.13, 6.91 (4CH, s), 7.93, 7.94 (2NH, m). (**Scheme 1**).

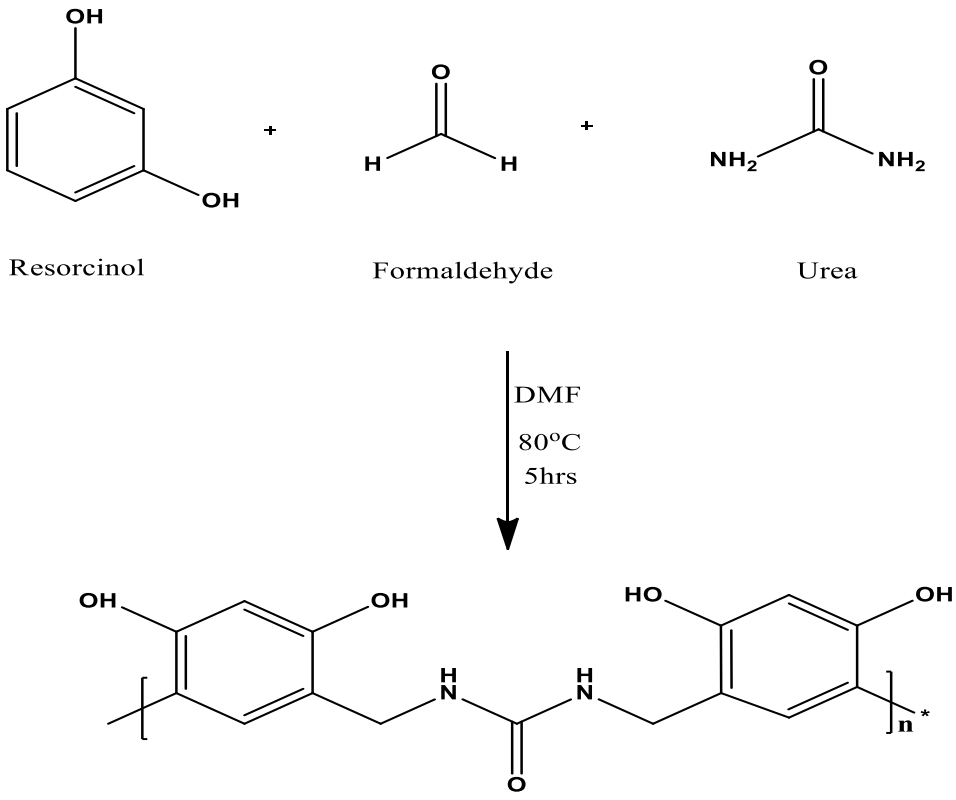

Scheme 1. Synthesis of the RFU terpolymer ligand.

Preparation of Polymer-Metal Complex

Formation of the copper (II) polymer-metal complex was carried out by the reaction of the terpolymer ligand (1.0 g) with copper (II) acetate (0.8 g) in a 1:1 molar ratio. These materials were dissolved in 15 ml and 10 ml ethanol respectively, and refluxed for 2 hours at 80 °C. A dark-green product was obtained, which was filtered off and oven dried at 40 °C (**Scheme 2**). Similar procedures were carried out for the formation of the other polychelates, RFU-Mn(II), RFU-Co(II), RFU-Ni(II), and RFU-Zn(II).

IR (film): RFU-Cu(II) 3632 cm^{-1}, 3445 cm^{-1} (υ N-H stretching), 3304 cm^{-1} (υ O-H stretching), 2937 cm^{-1} (υ C-H stretching), 1445 cm^{-1}, 1159 cm^{-1} (methylene bridge), 1344 cm^{-1} (in-plane bending δ OH), 1654 cm^{-1} (N-H bending), 1290 cm^{-1}, 958 cm^{-1} (sub. aromatic rings), 1568 cm^{-1} (υ C=O stretching), 607 cm^{-1} (υ O-M), 527 cm^{-1} (υ N-M). UV-Vis. 273 nm br. ^{1}H NMR (400 MHZ DMSO-d_6) δ [ppm]: 2.76 ($2CH_3$, s), 3.37 ($2CH_2$, s), 7.95 (4CH, m).

RESULTS AND DISCUSSION

FT-IR Analysis

The FT-IR spectra of the RFU resin and its metal complexes are shown in **Figure 1**. The peaks at 3515 cm^{-1}, 3437 cm^{-1}, and 3417 cm^{-1} were due to υ (N-H) stretching [21], while the peak at 3226 cm^{-1} was assigned to the υ (O-H) stretching of phenolic hydroxyl group [22-23]. A weak band which appeared at 2995 cm^{-1} was due to the υ (C-H) stretching of methylene group [24]. Peaks observed at 1407 cm^{-1}, and 1139 cm^{-1} were attributed to the methylene bridge linked to the aromatic ring [25]. The peak at 1321 cm^{-1} was assigned to an in-plane bending δ (OH) of the phenolic group [26], and another at 1640 cm^{-1} was attributed to the N-H bending of an amide group [27]. Tetra-substituted aromatic rings were assigned to the peaks at 1202 cm^{-1} and 971 cm^{-1}, while the peak at 1502 cm^{-1} was due to υ (C=O) stretching [28]. The spectra of polymer-metal complexes are characterized by the broadening and shifting of peaks, which are a feature of the chelation that occurs between the ligand and the metal ion [29]. In the RFU-Mn(II) complex, the C-NH peak appeared as a broad band recorded at 3692 cm^{-1}, while in the RFU-Co(II) complex, peaks were observed at 3556 cm^{-1}, 3487 cm^{-1}, and 3413 cm^{-1}, indicating a slight shift in peak positions compared to the RFU ligand. Similar behaviour was also observed in the C-OH peaks of the metal complexes of Co(II), Ni(II), and Cu(II). Absorption peaks at 682 cm^{-1} and 670 cm^{-1} in RFU-Cu(II) and RFU-Ni(II) were attributed to the rocking modes of water of coordination [30]. The presence of bands at 601-650 cm^{-1} and 433-

527 cm^{-1} supports the theory that chelation of the metal ion occurred through O and N [31-32]. The spectral bands observed for the RFU terpolymer ligand and its metal complexes are listed in **Table 1**.

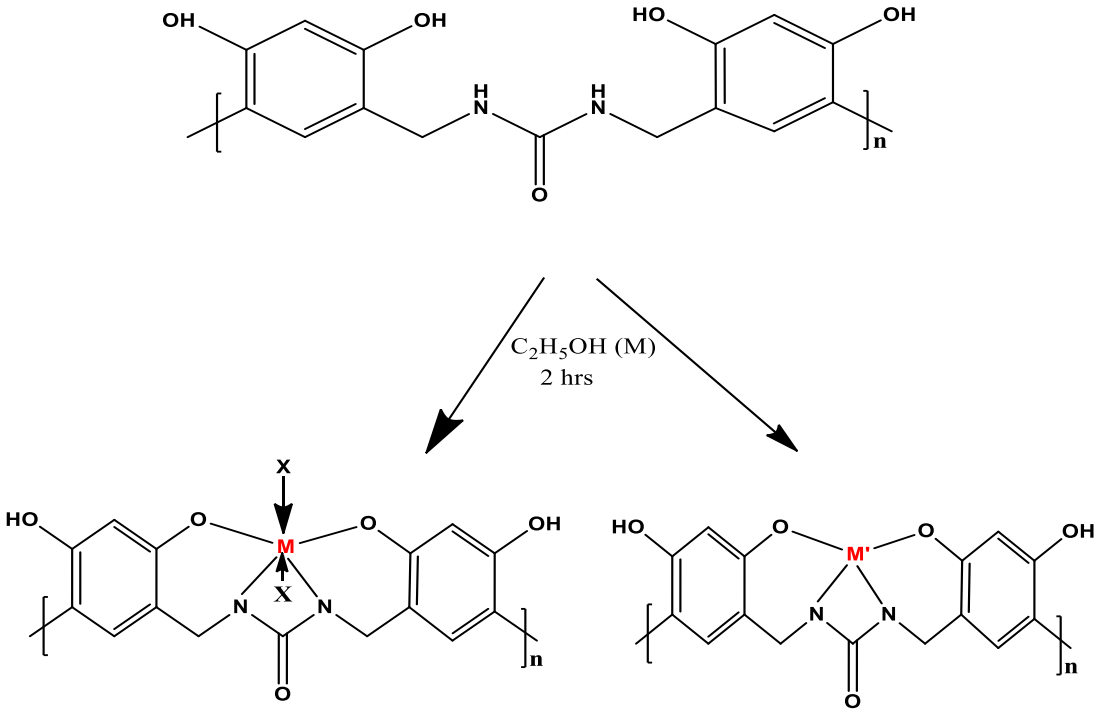

RFU-M terpolymer metal complexes

M = Mn (II), Co (II), Ni (II)
X = H_2O

M' = Cu(II), Zn(II)

Scheme 2. Synthesis of RFU terpolymer-metal complexes.

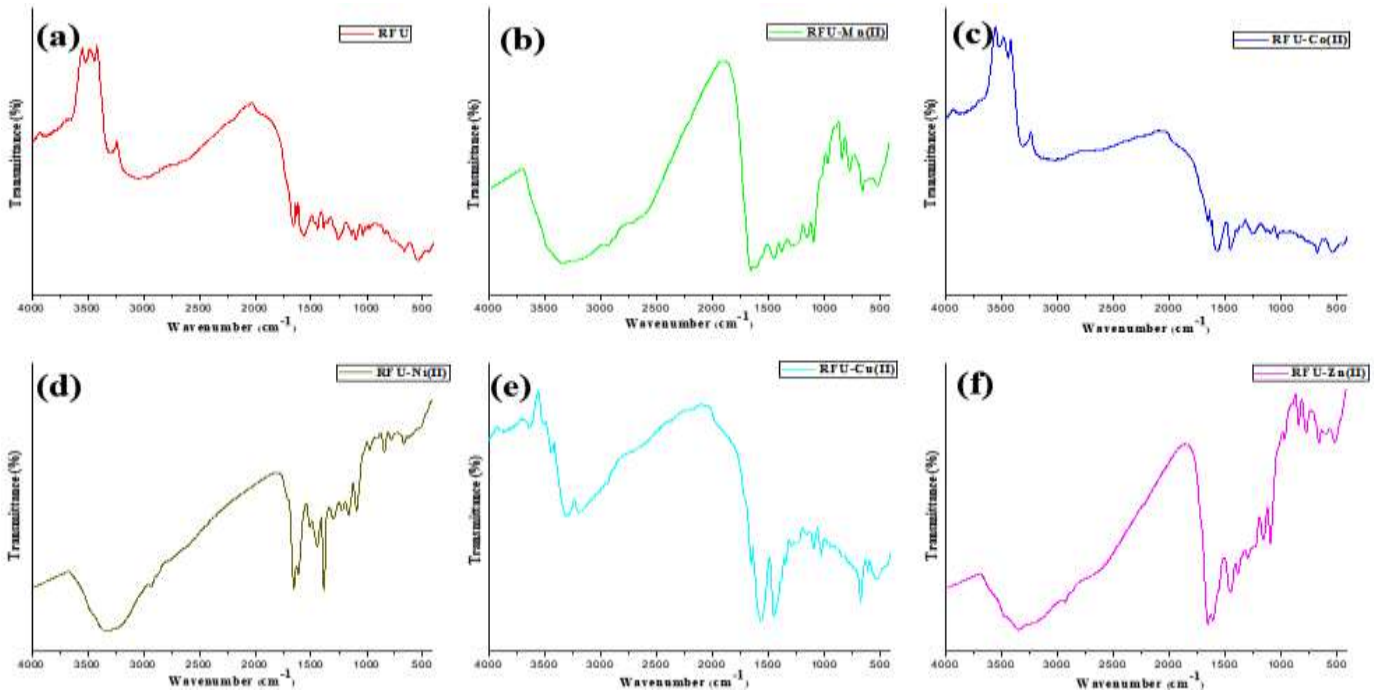

Figure 1. FTIR analysis.

Table 1. FTIR spectral data of RFU terpolymer and its metal complexes

Assignment	Wavenumber (cm^{-1})					
	RFU	**RFU-Mn(II)**	**RFU-Co(II)**	**RFU-Ni(II)**	**RFU-Cu(II)**	**RFU-Zn(II)**
υ (N-H) stret	3515, 3437, 3417	3692	3556, 3487, 3413	-	3632, 3445	-
υ (O-H) stret	3226	-	3237	3296	3304	3351
υ (C-H) stret	2995	2927	2992	2922	2937	2922
$-CH_2-$	1407, 1139	1407, 1159	1409, 1132	1438, 1159	1445, 1159	1456, 1153
δ (O-H) bend	1321	1321	1321	1383	1344	1375
δ (N-H) bend	1640	1625	1633	1656	1654	1657
Subt. Ar. Ring	1202, 971	1260, 971	1253	1290, 964	1290, 958	1290, 964
C=O	1502	1508	1506	1508	1568	1595
υ (O-M)	-	645	527	607	607	601
υ (N-M)	-	514	433	514	527	514

Electronic Spectra

Electronic spectra of the RFU ligand and its metal complexes (**Figure 2**) were recorded in DMSO. The RFU ligand showed a broad band at 285 nm (35087 cm^{-1}) and a small band at 540 nm (18518 cm^{-1}), attributed to the π→π* [33] and n→π* [34] transitions, respectively. Upon chelation, all the complexes underwent a blue shift, exhibiting absorption bands from 259 nm (38610 cm^{-1}) to 284 nm (35211 cm^{-1}). The manganese complex peak at 259 nm (38610 cm^{-1}) was due to a π→π* transition [35], while the peak at 282 nm (35460 cm^{-1}) demonstrated by the cobalt complex was also due to a π→π* transition [36]. In the nickel and copper complexes, peaks recorded at 284 nm (35211 cm^{-1}) and 273 nm (36630 cm^{-1}) respectively were attributed to π→π* transitions [37] [38]. The zinc complex was diamagnetic, as reported previously [39].

XRD

XRD patterns of the synthesized RFU terpolymer and its metal complexes are shown in **Figure 3**. The resin demonstrated a broad band at 2-theta = 22°, and the absence of other diffraction peaks was attributed to the amorphous nature of the material. Different peaks were observed with the incorporation of various metal ions, with RFU-Mn(II), RFU-Co(II), and RFU-Ni(II) displaying semi-crystalline attributes. For RFU-Cu(II), well-defined crystalline behaviour (based on the sharp peaks) was observed, while RFU-Zn(II) maintained its amorphous property with 2-theta recorded at 21°.

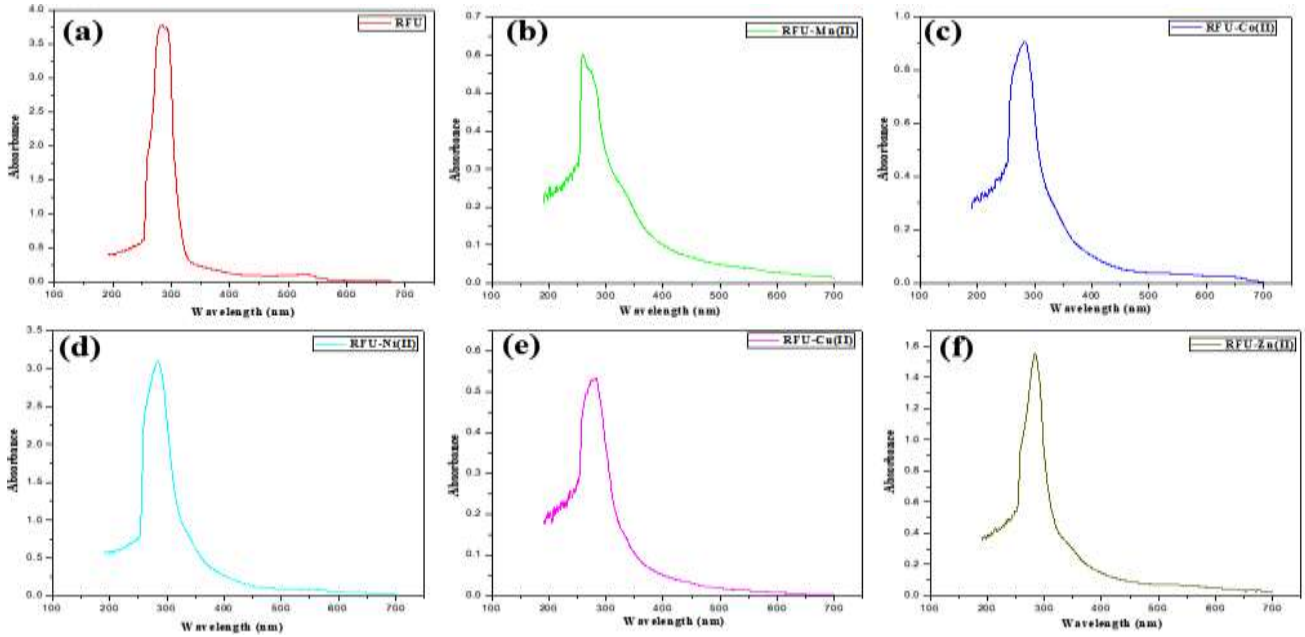

Figure 2. Electronic spectra.

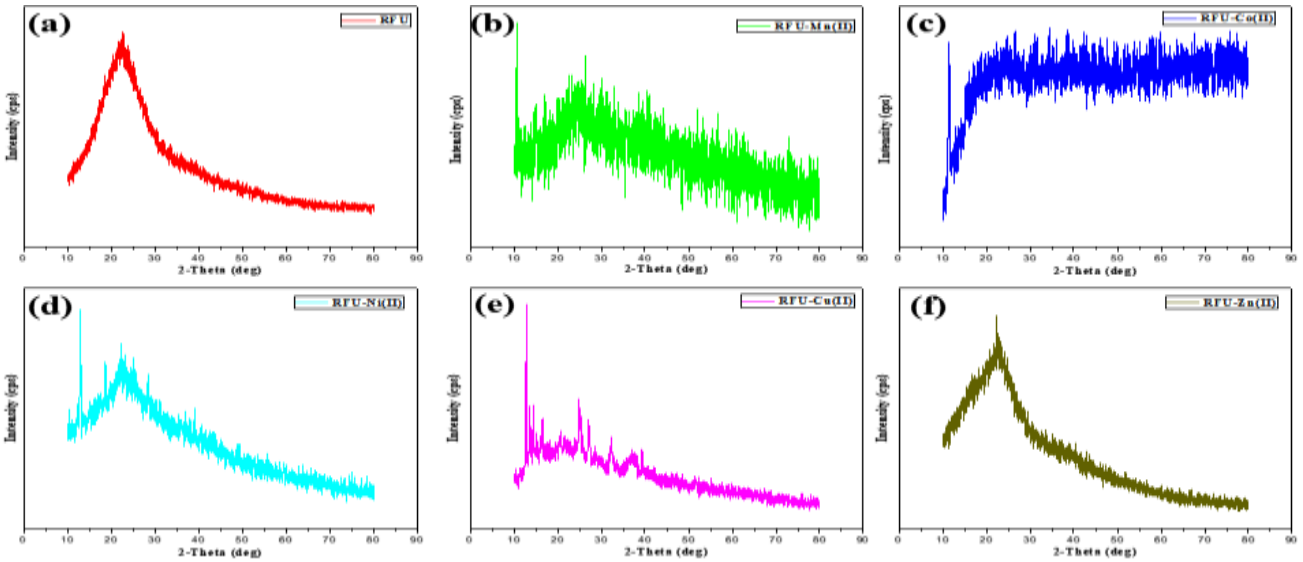

Figure 3. XRD diffraction patterns.

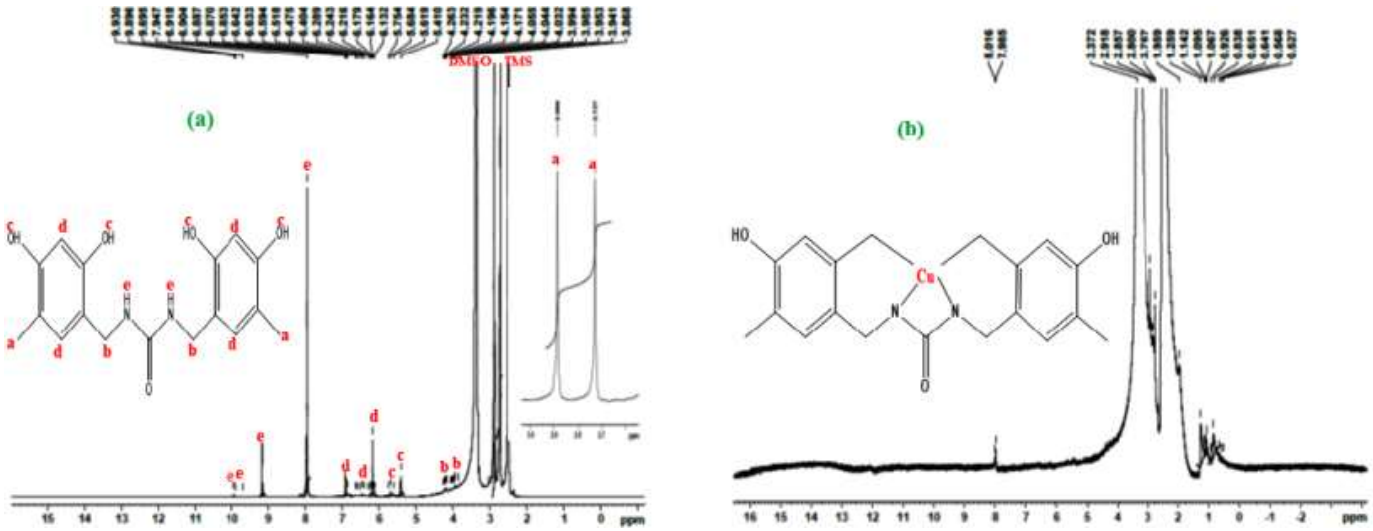

Figure 4. ^{1}H NMR spectra.

^{1}H NMR

The proton NMR spectra of the terpolymer ligand (RFU) and its copper (II) complex are shown in **Figure 4a**. The peaks at 2.72 ppm and 2.88 ppm were due to methyl groups [40]. Methylene peaks were observed at 4.03-4.26 ppm [41], while the OH peaks were present at 5.41-5.75 ppm [42]. The CH aromatic peaks were at 6.13-6.91 ppm [43], while the other observed peaks at 7.93-7.94 ppm were attributed to NH amide [44]. In RFU-Cu (**Figure 4b**), the peaks appeared broad and disoriented when compared to the RFU ligand (**Figure 4a**). In addition, there was a complete disappearance of the hydroxyl peaks at 5.41-5.7 ppm, and a partial disappearance of the NH peaks. These characteristics are attributed to the chelation that took place between the OH/NH groups and the copper ion, as established previously [45].

SEM

SEM analysis results for the RFU resin and its metal polychelates are shown in **Figure 5**, and it was observed that the materials possessed different morphologies. The RFU resin (**Figure 5a**) had a smooth surface with little space in between, and the arrangement pattern was irregular. A spongy-like appearance was seen in the Mn(II) complex (**Figure 5b**), while Co(II) complex (**Figure 5c**) had an ice cube-like structure arranged in a regular pattern. The Ni(II) complex (**Figure 5d**) possessed a cotton-like appearance, and the Cu(II) complex (**Figure 5e**) looked like a bird filler with some needle-like structures. In the case of the Zn(II) complex (**Figure 5f**), both smooth and rough surfaces were observed, as well as needle-like features.

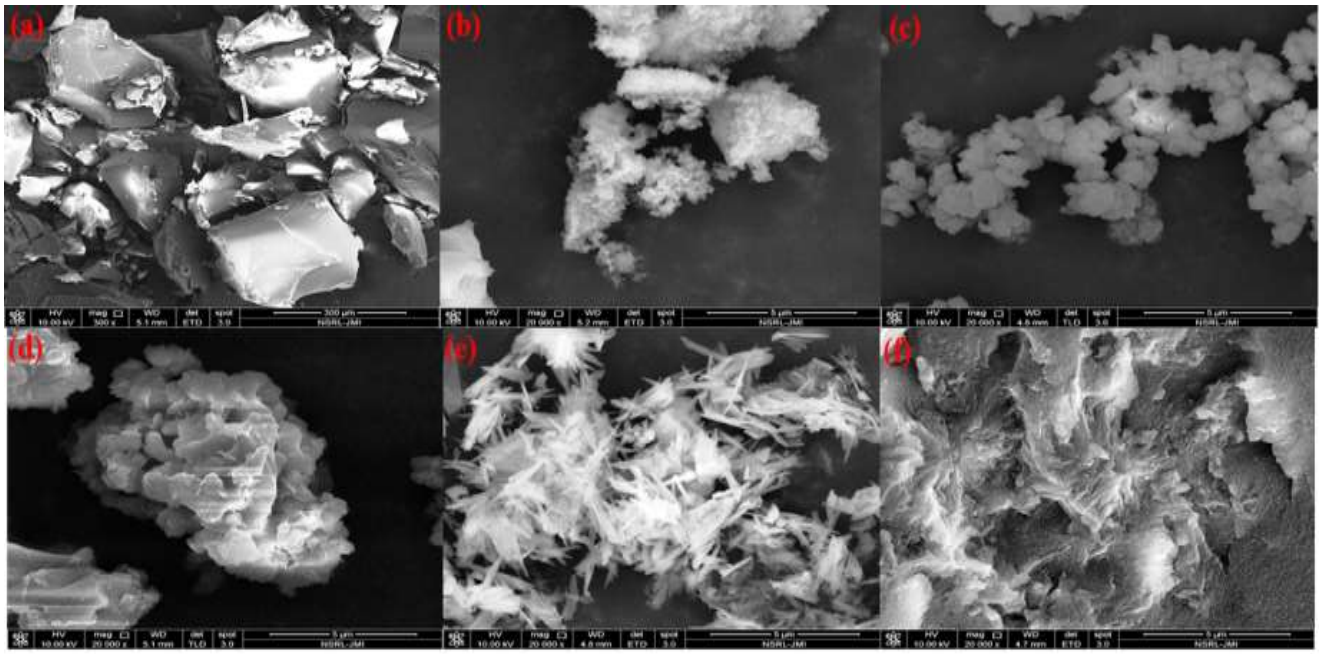

Figure 5. SEM images.

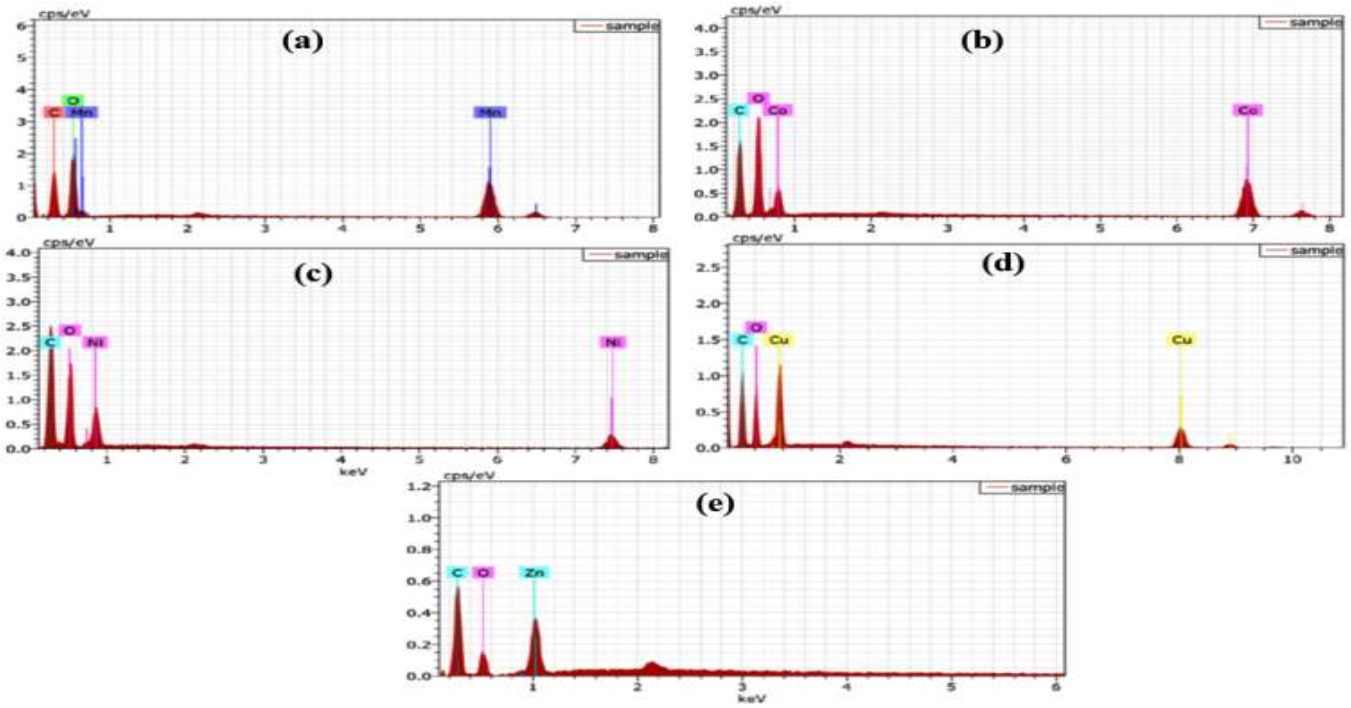

Figure 6. EDX spectra.

EDX

EDX spectra of the synthesized materials (**Figure 6**) showed the presence of elemental carbon and oxygen, as well the atomic percentage of metal complexes which confirmed their binding with the ligand. The atomic percentages of the polychelates recorded were: Mn (6.57), Co (5.83), Ni (1.99), Cu (5.47), and Zn (6.27).

TGA

The results of the TGA analysis of the terpolymer (RFU) and its metal complexes are depicted in **Figure 7**. Based on the thermogram, the resin had undergone a two-step degradation process. The first degradation was observed at 191 °C (corresponding to 15% weight loss) attributed to the loss of solvent or water or gas desorption [46]. The second degradation was seen at

362 °C, which resulted in thermoxidative decomposition of the material [47]. The resin was characterized by drastic weight loss, thus at 600 °C it had only 18 % of its weight left. The Mn, Co, and Zn metal complexes) also underwent a two-step degradation process. The manganese complex degraded at 195 °C, and 341 °C, while the cobalt complex degraded at 197 °C and 336 °C. The first phase of degradation in the zinc complex was observed at 200 °C, and the second phase at 396 °C, which indicates the stability of the zinc complex compared to the other complexes. On the other hand, the Ni and Cu complexes were characterized by three-step degradation patterns. The nickel (II) complex recorded degradation at 216 °C, 291 °C, and 340 °C. Similarly, the copper (II) complex degraded at 183 °C, 264 °C, and 350 °C. These degradation phases can be assigned to solvent loss, first decomposition products, and thermal onset. It is worth mentioning that the formation of oxides (MnO, CoO, NiO, CuO, ZnO) are among the attributes of these materials after their final decomposition [48]. It can be deduced from the thermogram that the nickel and copper complexes possessed more thermal stability based on their degradation steps. On the other hand, considering the weight left at the end of the process (600 °C), the zinc and cobalt complexes are more promising. The characteristic weight loss data for the terpolymer and its metal complexes are listed in **Table 2**.

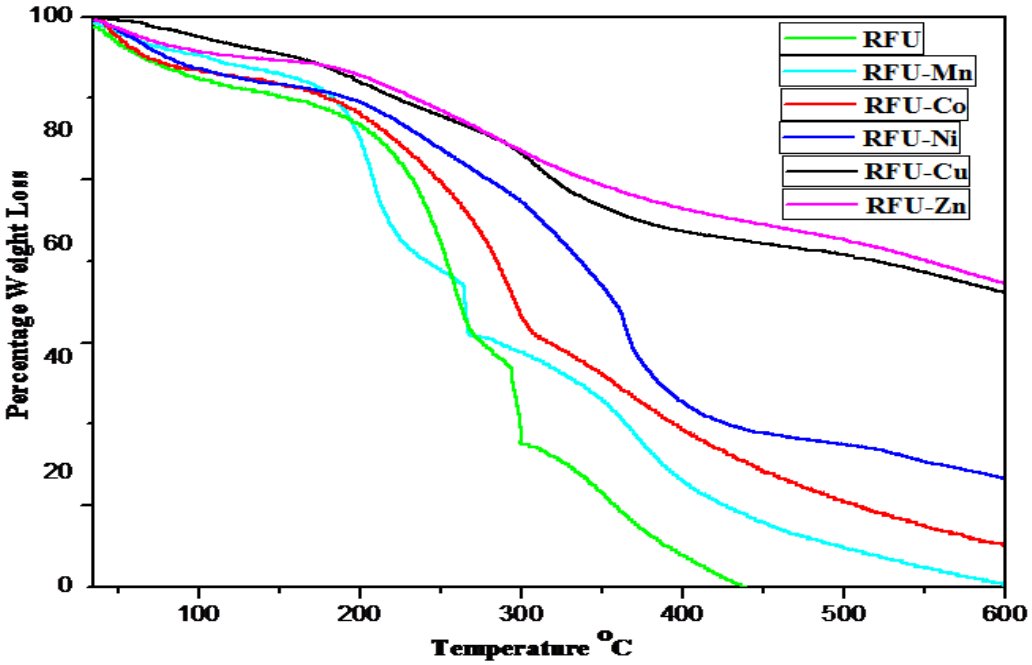

Figure 7. TGA results.

Table 2. Characteristic weight loss of RFU terpolymer and its metal complexes

Compounds	Weight (%) left at the indicated temperature (ºC)					Characteristic weight (%) left at 600 ºC
	100	200	300	400	500	
RFU	90	85	68	31	24	18
RFU-Mn(II)	93	87	62	49	39	35
RFU-Co(II)	95	87	75	61	57	51
RFU-Ni(II)	92	85	47	33	25	22
RFU-Cu(II)	95	84	58	42	34	30
RFU-Zn(II)	94	89	76	66	60	53

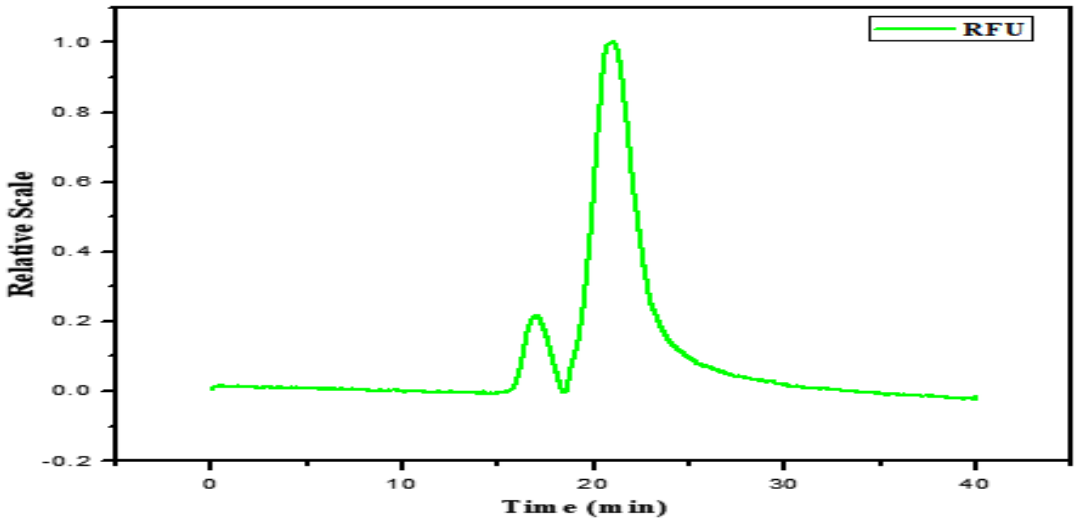

Figure 8. GPC analysis of RFU.

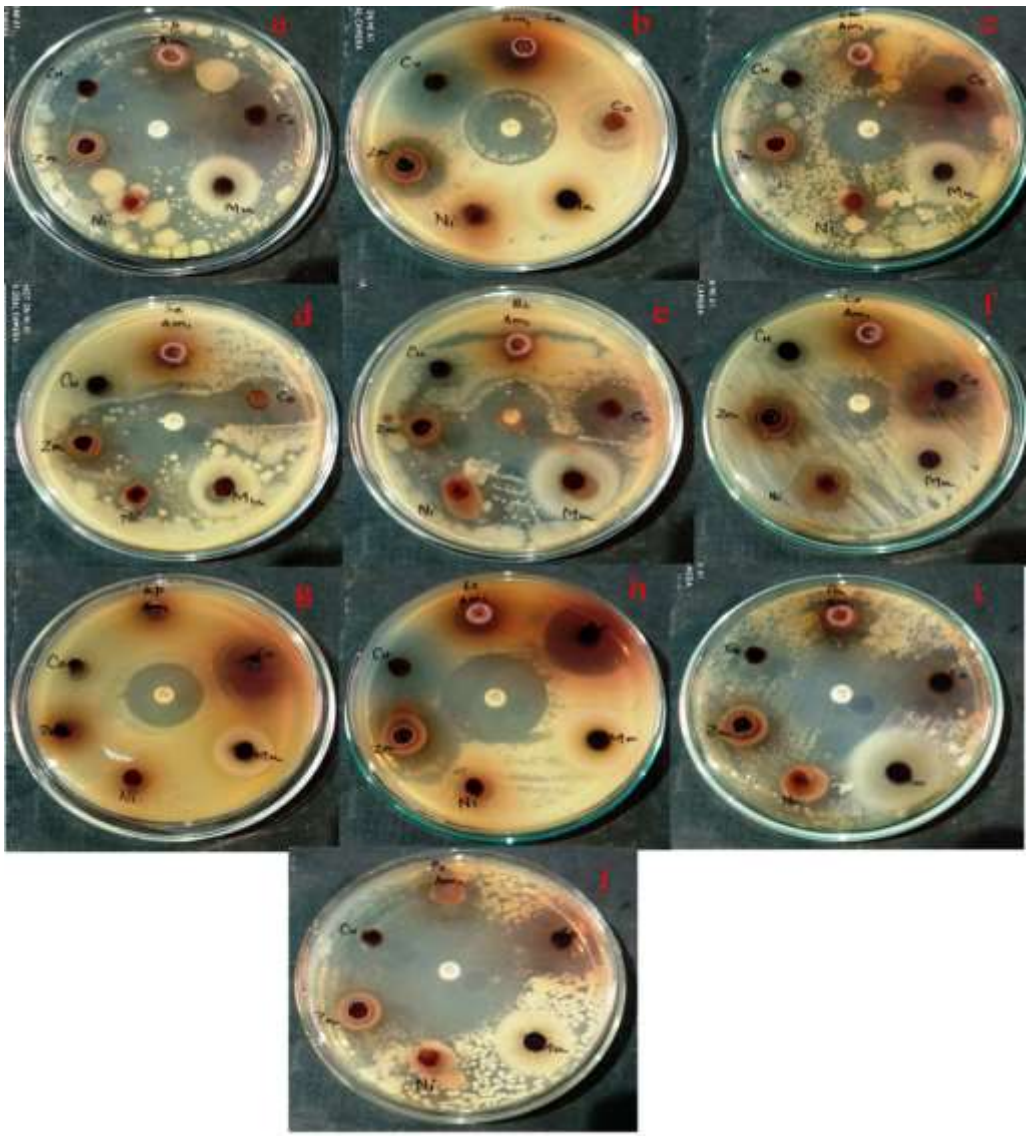

Figure 9. Agar diffusion test.

GPC

Gel permeation chromatography (GPC), often referred to as size-exclusion chromatography (SEC), has been applied in the determination of molecular weight distribution or molecular mass characterization of polymeric materials [49-50].

Results of the GPC analysis of the terpolymer RFU ligand are shown in **Figure 8**. The analysis gave the number average molecular weight (M_n) as 8900, weight average molecular weight (M_w) as 17700, and poly dispersity index (PDI) as 1.985.

Antibacterial Activity

The antibacterial activity (**Figure 9**) of RFU and its metal complexes was determined through agar diffusion tests, and the results are given in **Table 3** and **Figure 10**. The RFU-Co(II) complex showed strong antibacterial activity against *S. mutans* (27 mm), *B. cerus* (24 mm), *E. coli* (18 mm), and *K. pneumoniae* (19 mm). Thus, in all the aforementioned bacteria, the cobalt complex was more effective than the standard drugs (ciprofloxacin and gentamicin). The other complexes of Mn, Co, Ni, Cu, and Zn also demonstrated antibacterial activity. The inhibition behaviour of the complexes was due to the presence of O and N donor groups which affect the production of enzymes that require a free hydroxyl group [51-52]. The RFU resin also showed sensitivity to bacteria (except *K. pneumonia*e), which can be attributed to the polymer that acts as a matrix of material by holding antimicrobial agents [53, 54].

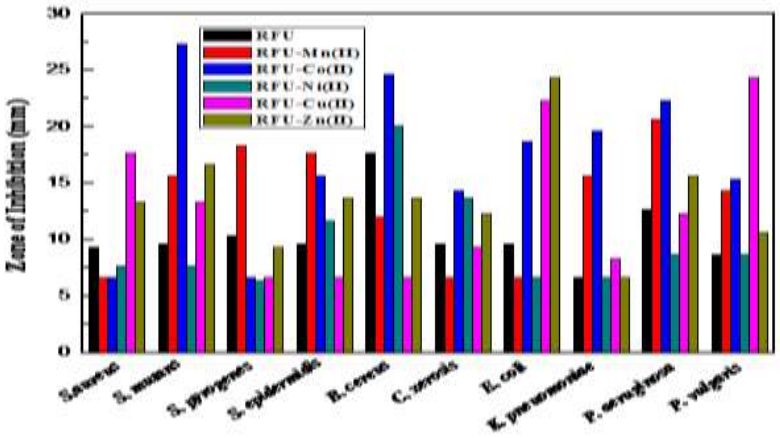

Figure 10. Graphical representation of antibacterial activity.

Figure 11. Antifungal activity test.

Table 3. Antibacterial activity of test samples showing the zones of inhibition (in mm).

	RFU	RFU-Mn(II)	RFU-Co(II)	RFU-Ni(II)	RFU-Cu(II)	RFU-Zn(II)	Positive Control[2]
Staphylococcus aureus	9.33±0.33 (0.57) S	6.66±0.33 (0.57) R	6.66±0.33 (0.57) R	7.66±0.66 (1.15) S	17.66±0.57 (1.0) S	13.33±0.57 (1.0) S	24.33±0.33 (0.57) S
Streptococcus Mutans	9.66±0.33 (0.57) S	15.66±0.33 (0.57) S	27.33±0.57 (1.0) S	7.66±0.66(1.15) S	13.33±0.57 (1.0) S	16.66±0.33 (0.57) S	17.66±0.88 (1.5) S
Staphylococcus pyrogenes	10.33±0.57 (1.0) S	18.33±0.33 (0.57) S	6.66±0.33 (0.57) R	6.33±0.33 (0.57) R	6.66±0.33 (0.5) R	9.33±0.63 (1.15) S	39.33±0.66 (1.15) S
Staphylococcus epidermidis	9.66±0.33 (0.57) S	17.66±0.33 (0.57) S	15.66±0.33 (0.57) S	11.66±0.33 (0.57) S	6.66±0.33 (0.57) R	13.66±0.66 (1.15) S	25.66±0.33 (0.57) S
Bacillus cereus	17.66±0.66 (1.15) S	12.0±0.57 (1.0) S	24.66±0.33 (0.57) S	20.06±0.57 (1.0) S	6.66±0.33 (0.5) R	13.66±0.66 (1.15) S	21.33±0.66 (1.15) S
Corynebacterium xerosis	9.66±0.33 (0.57) S	6.66±0.33 (0.57) R	14.33±0.57 (1.0) S	13.66±0.57 (1.0) S	9.33±0.63 (1.15) S	12.33±0.33 (0.57) S	17.33±0.33 (0.57) S
Escherichia coli	9.66±0.33 (0.57) S	6.66±0.33 (0.57) R	18.66±0.66 (1.15) S	6.66±0.33 (0.57) R	22.33±0.33 (0.57) S	24.33±0.57 (1.0) S	17.66±0.33 (0.57) S
Klebseilla pneuomoniae	6.66±0.33 (0.57) R	15.66±0.33 (0.57) S	19.66±0.57 (1.0) S	6.66±0.33 (0.57) R	8.33±0.33 (0.57) S	6.66±0.33 (0.57) R	18.66±0.33 (0.57) S
Pseudomonas aeruginosa	12.66±0.66 (1.15) S	20.66±0.33 (0.57) S	22.33±0.33 (0.57) S	8.66±0.33 (0.57) S	12.33±0.57 (1.0) S	15.66±0.33 (0.57) S	29.33±0.33 (0.57) S
Proteus vulgaris	8.66±0.33 (0.57) S	14.33±0.57 (1.0) S	15.33±0.33 (0.57) S	8.66±0.33 (0.57) S	24.33±0.57 (1.0) S	10.66±0.33 (0.57) S	39.33±0.33 (0.57) S

[1] - Dimethyl Sulphoxide

[2] - Standard Drug (Ciprofloxacin for Gram-positive and Gentamicin for Gram-negative strains)

Results expressed as Mean ± Standard error of Mean (Standard Deviation)

S -Sensitive R- Resistant

Antifungal Activity

The antifungal activity (Figure 11) of the RFU and its metal complexes was determined through the well diffusion method, using casitone agar. All the synthesized materials showed no activity towards *A. niger, C. albicans, P. notatum,* and *S. cerevisiae.* This behaviour could be attributed to less cell permeability, fitness of the particle size of the metal ion, and the existence of large organic moieties [55, 56].

CONCLUSION

The RFU terpolymer and its metal complexes were synthesized and characterized by various techniques. The formation of terpolymer-metal complexes resulted in enhanced properties such as thermal stability and antibacterial activity. The RFU-Co(II) complex should be further investigated as a potential antibacterial agent.

ACKNOWLEDGEMENTS

The authors are grateful to the CIF of Jamia Millia Islamia for providing the characterization facilities, SAIF IIT Madras for providing the ^{1}H NMR facility, and Professor Sultan A Nasar of the Polymer Science Department, University of Madras, for GPC analysis.

REFERENCES

1. Pol, V. G., Shrestha, L. K., and Ariga, K. (2014) Tunable, Functional Carbon Spheres Derived from Rapid Synthesis of Resorcinol-Formaldehyde Resins. *Applied Materials and Interfaces*, **6**, 10649–10655.

2. Shiraishi, Y., Takii, T., Hagi, T., Mori, S., Kofuji, Y., Kitagawa, Y., Tanaka, S., Ichikawa, S. and Hirai, T. (2019) Resorcinol–formaldehyde resins as metal-free semiconductor photocatalysts

for solar-to-hydrogen peroxide energy conversion. *Nature Materials*, **18**, 985–993.

3. Friscic, T., Jones, W. (2010) Benefits of cocrystallisation in pharmaceutical materials science: an update. *Pharmacy and Pharmacology*, **62**, 1547–1559.

4. Hedaoo, R. K., Mahulikar, P. P. and Gite, V. V. (2013) Synthesis and Characterization of Resorcinol-Based Cross Linked Phenol Formaldehyde Microcapsules for Encapsulation of Pendimethalin. *Polymer-Plastics Technology and Engineering*, **52**, 243–249.

5. Ito, F., Fusegi, K., Kumamoto, T., and Ishikawa, T. (2007) Boron trichloride mediated regioselective claisen rearrangement of resorcinol derivatives: Application to resorcinol carvonyl, ethers. *Synthesis*, **12**, 1785–1796**.**

6. Adachi, O., Fujii, Y., Ghaly, M. F., Toyama, H., Shinagawa, E., and Matsushita, K. (2001) Membrane-bound Quinoprotein D-Arabitol Dehydrogenase of Gluconobacter suboxydans IFO 3257: A Versatile Enzyme for the Oxidative Fermentation of Various Ketoses. *Bioscience Biotechnology and Biochemistry*, **65**, 2755–2762.

7. Kilinc, N. (2022) Resorcinol Derivatives as Novel Aldose Reductase Inhibitors: In *silico* and In *vitro* Evaluation. *Letters in Drug Design and Discovery*, **9**, 837–846.

8. Lee, W. –J., Lan, W. -C. (2006) Properties of resorcinol–tannin–formaldehyde copolymer resins prepared from the bark extracts of Taiwan acacia and China fir. *Bioresource Technology*, **97**, 257–264.

9. Bregovic, V. B., Basaric, N. and –Majerski, K. M. (2015) Anion binding with urea and thiourea derivatives. *Coordination Chemistry Review*, **295**, 80–124**.**

10. Weiner, I. D., Mitch, W. E., and Sands, J. M. (2015) Urea and Ammonia Metabolism and the Control of Renal Nitrogen Excretion. *American Society of Nephrology*, **10**, 1444–1458.

11. Raval, D. K., Narola, B. N. and Patel, A. J. (2005) Synthesis, Characterization and Composites from Resorcinol-urea-formaldehyde-casein Resin. *Iranian Polymer Journal*, **9**, 775–784.

12. Khakimov, M. S., Gazizov, A. S., Burilov, A. R., Pudovik, M. A., and Konovalov, A. I. (2009) Reaction of resorcinol and its derivatives with urea acetals. *Russian Journal of General Chemistry*, **79**, 1163.

13. Yu, J., Guo, M., Muhammad, F., Wang, A., Zhang, F., Li, Q. and Zhu, G. (2014**)** One-pot synthesis of highly ordered nitrogen-containing mesoporous carbon with resorcinol–urea–formaldehyde resin for CO_2 capture. *Carbon*, **69**, 502–514.

14. Azarudeen, S. R., Ahamed, R. A. M., Jeyakumar, D. and Burkanudeen, R. A. (2009) An Eco-friendly Synthesis of a Terpolymer Resin: Characterization and Chelation Ion-exchange Property. *Iranian Polymer Journal*, **18**, 821–832.

15. Verma, B. C., Quraishi, A. M. and Ebenso, E. E. (2013) Electrochemical and Thermodynamic Investigation of Some Soluble Terpolymers as effective corrosion inhibitors for Mild Steel in 1M hydrochloric acid solution. *International Journal of Electrochemical Science*, **8**, 12894–12906.

16. Hussein, H. E., Safa, S. H., Samar, A. A. and Ehab, M. A. (2022) Synthesis, Characterization, PXRD studies, Theoritical calculation, and Antitumor Potency studies of a Novel N,O,-Multidentate chelating ligands and its Zr(IV), V(IV), Ru(IV), and Cd(II) complexes. *Bioinorganic Chemistry and Applications*, 2022.

17. Amaury, M. H., Stephane, T. G. S., and Jean, -L. P. (2006) Design of Iron chelators: Synthesis and Iron (II) complexing abilities of tripodal tris-bidentate ligands. *Biometals*, **19**, 349–366.

18. Noormohamadi, H. R. Fathi, M. R. Ghaedi, M. Azizzadeh, S. and Nobakht, V. (2018) Mechano-chemically synthesized Ag (I) coordination polymer as a new adsorbent and its application to ultrasound assisted wastewater treatment via the central composite design: Isotherm and kinetic studies. *Molecular Liquids*, **262**, 71–77.

19. Balouiri, M., Sadiki, M. and Ibnsouda, S. K. (2016) Methods for *in vitro* evaluating anti-microbial activity: A review. *Pharmaceutical Analysis*, **6**, 71–79.

20. Katkamwar, S. S., Zade, A. B., Rahangdale, S. S. and Gurnule, W. B. (2009) Terpolymer resin–III: Synthesis and characterization of 8-hydroxyquinoline–dithiooxamide–formaldehyde terpolymer resins. *Applied Polymer Science*, **33**, 3330–3335**.**

21. Oswald, O., Suhm, M. A. and Coussan, S. (2019) Incremental NH stretching downshift through stepwise nitrogen complexation of pyrrole: a combined jet expansion and matrix isolation study. *Physical Chemistry Chemical Physics*. **21**, 1277.

22. Mikhaylova, Y., Adam, G., Haussler, L., Eichhorn, K. -J. and Voit, B. (2006) Temperature-dependent FTIR spectroscopic and thermoanalytic studies of hydrogen bonding of hydroxyl (phenolic group) terminated hyperbranched aromatic polyesters. *Molecular Structure*, **788**, 80–88.

23. Jianwei, F., Zhonghui, C., Minghuan, W., Shujan, L., Jianghui, Z., Jianan, Z., Runping, H. and Qun, X. (2015) Adsorption of methylene blue by a high-efficiency adsorbent (polydopamine microspheres): Kinetics, isotherm, thermodynamics and mechanism analysis. *Chemical Engineering Journal*, **259**, 53–61.

24. Lu, R., Gan, W., Wu, B., Zhang, Z., Guo, Y. and Wang, H. (2005) C−H Stretching Vibrations of Methyl, Methylene and Methine Groups at the Vapor/Alcohol (n = 1−8) Interfaces. *Physical Chemistry B*, **109**, 14118–14129.

25. Nilgun, K., Pelin, D. (2013) In *situ* modification of cyclohexanone formaldehyde resin with boric acid for high performance application. *Applied Polymer Science*, **129**, 2813–2820.

26. Zghari, B., Hajji, L., Boukir, A., (2018) Effect of moist and dry heat weathering conditions on cellulose degradation of historical manuscripts exposed to accelerated ageing: 13C NMR and FTIR spectroscopy as non-invasive monitoring approach. *J. Materials Environmental Science*, **9**, 641–654.

27. Diana, J. P., Grace, L., Fitria, S. (2017) Interpretation of FTIR spectrum of seawater and sediment in the Ambon Bay (TAD). *AIP Conference Proceedings*, **1801**, 060005.

28. Yang, H., Yan, R. Chen, H., Lee, D. H. and Zheng, C. (2007) Characteristics of hemicellulose, cellulose and lignin pyrolysis. *Fuel*, **86**, 1781–1788**.**

29. Wu, K. H., Wang, Y. R. and Hwu, W. H. (2003) FTIR and TGA studies of poly(4-vinylpyridine-*co*-divinylbenzene)–Cu(II) complex. *Polymer Degradation and Stability*, **79**, 195–200.

30. Stoilova, D., Koleva, V. (2000) IR study of solid phases formed in the $Mg(HCOO)_2$–$Cu(HCOO)_2$–H_2O system. *Molecular Structure*, **553**, 131–139.

31. Gupta, K. C., Sutar, A. K. (2008) Synthesis of polymer-supported metal-ion complexes and evaluation of their catalytic activities. *Applied Polymer Science*, **108**, 3927–3941.

32. Singh, M. K., Das, A. and Paul, B. (2009) Synthesis and characterization of mixed ligand complexes of cobalt(II) with some nitrogen and sulfur donors. *Coordination Chemistry*, **62**, 2745–2754.

33. Yang, J., Tang, R., Shi, S. J. and Nie, J. (2013) Synthesis and characterization of polymerizable one-component photoinitiator based on sesamol. *Photochemistry Photobiology Science*, **12**, 923–929.

34. Skrabania, K., Miasnikova, A., –Koumba, A. M. B., Zhem, D., and Laschewsky, A. (2011) Examining the UV-vis absorption of RAFT chain transfer agents and their use for polymer analysis. *Polymer Chemistry*, **2**, 2074–2083.

35. Verma, S. K., Singh, V. K. (2014) One pot three component synthesis of mononuclear [M(1,1-dithiolato)$_2$] {Mn(II), Co(II), Zn(II) and Cd(II)} complexes, spectral characterization, fluorescence, optical and thermogravimetric study. *Polyhedron*, **76**, 1–9.

36. Ramachandran, E., Thomas, S. P., Poornima, P. Kalaivani, P., Prabhakaran, R., Padma, V. V. and Natarajan, K. (2012) Evaluation of DNA binding, antioxidant and cytotoxic activity of mononuclear Co(III) complexes of 2-oxo-1,2-dihydrobenzo[h] quinoline-3-carbaldehyde thiosemicarbazones. *European Journal of Medicinal Chemistry*, **50**, 405–415.

37. Shahabadi, N., Fatahi, A. (2010) Multi-spectroscopic DNA-binding studies of a tris-chelate nickel(II) complex containing 4,7-diphenyl 1,10-phenanthroline ligands. *Molecular Structure*, **970**, 90–95**.**

38. Zhang, S., Zhu, Y., Tu, C., Wei, H., Yeng, Z., Lin, L., Ding, J., Zhang, J. and Guo, Z. (2004) A novel cytotoxic ternary copper(II) complex of 1,10-phenanthroline and L-threonine with DNA nuclease activity. *Inorganic Biochemistry*, **98**, 2099–2106.

39. Neelakantan, M. A., Marriappan, S. S., Dharmaraja, J., Jeyakumar, T. and Muthukumaran, K. (2008) Spectral, XRD, SEM and biological activities of transition metal complexes of polydentate ligands containing thiazole moiety. *Spectrochimica Acta A*, **71**, 628–635.

40. Knothe, G., Kenar, J.A. (2004) Determination of the fatty acid profile by ^{1}H-NMR spectroscopy, *European Journal of Lipid Science and Technology*, 106, 88–96.

41. Wu, Z., Sung, B. and Butler, I. S. (2012) Optimized structures and Theoritical ^{1}H-NMR spectral analysis of methylene protons in Dibenzylnsulfoxide. *Advanced Materials Research*, 391–392, 1368–1374.

42. Ahmad, S., Gupta, A. P., Sharmim, E., Alam, M., Pandey, S. K. (2005) Synthesis, Characterization and development of high performance siloxane-modified epoxy paints. *Progress in Organic Coatings*, **54**, 248–255.

43. Catenescu, O., Grigoras, M., Colotin, G., Dobreanu, A., Hurduc, N. and Simionescu, C. I. (2001) Synthesis and characterization of some aliphatic–aromatic poly(Schiff base)s. *European Polymer Journal*, **37**, 2213–2216.

44. Yuting, W., Wei, Z., Ranran, J., Yifu, Y. and Bin, Z. (2020) Unveiling the activity origin of copper-based electrocatalyst for selective nitrate reduction to ammonia. *Angewandte Chemie International Edition*, **59**, 5350–5354.

45. Dharmaraj, N. (2001) Ruthenium(II) complexes containing bidentate Schiff bases and their antifungal activity. *Transition Metal Chemistry*, **26**, 105–109.

46. Maria, S. -Z. (2001) Thermal degradation of copolymers of styrene with dicarboxylic acids alternating styrene-maleic acid copolymer. *Polymer Degradation and Stability*, **74**, 579–584.

47. Corres, M. A., Zubitur, M., Cortazar, M. and Mugica, A. (2011) Thermal and thermo-oxidative degradation of poly(hydroxy ether of bisphenol-A) studied by TGA/FTIR and TGA/MS. *Analytical and Applied Pyrolysis*, **92**, 407–416**.**

48. Everson, K., Jeanne, M. H. (2006) Thermal degradation of acetate-intercalated hydroxyl double and hydroxy salts. *Inorganic Chemistry*, **9**, 3766–3773.

49. Edouard, S. P. B., Stephan, M. K. (2014) Advances in size-exclusion seperations of proteins and polymers by UHPLC. *Trend in Analytical Chemistry*, **63**, 85–94.

50. Laszlo, G., Tuan, Q. N., Christopher, J. G. P., Jan-Anders, E. M. (2003) Characterization of Hyperbranched Aliphatic Polyester and their trimethylsilylated derivatives by GPC-Viscometry, *Liquid Chromatography & Related Technologies*, **26**, 207–230.

51. Chohan, Z. H., Pervez, H., Rauf, A., Khan, K. M. and Supuran, C. T. (2004) Isatin-derived Antibacterial and Antifungal Compounds and their Transition Metal Complexes. *Enzyme Inhibition and Medicinal Chemistry*, **19**, 417–423.

52. Beheshti, A., Fard, M. S. E., Kubicki, M., Mayer, P., Abrahams, T. C. and Razatofighi, E. S. (2019) Design, synthesis and characterization of copper-based coordination compounds with bidentate (N,N and N,O) ligands: reversible uptake of iodine, dye adsorption and assessment of their antibacterial properties. *Crystal Engineering Communication*, **21**, 251–262.

53. Bonilla, A. M., and Garcia, M. F. (2012) Polymeric materials with antimicrobial activity. *Progress in Polymer Science*, **37**, 281–339.

54. Amin, M. K., Sayed, M. B. H. and Sara, L. (2018) Antimicrobial agents and packaging systems in antimicrobial active food packaging: An overview of approaches and interactions. *Food and Bioproducts Processing*, **111**, 1–19.

55. Tadari, S. K., Yadav, A. A. and Bendre, R. S. (2018) Synthesis and characterization of a novel schiff base of 1,2-diaminopropane with substituted salicyaldehyde and its transition metal complexes: Single crystal structures and biological activities. *Molecular Structure*, **1152**, 223–231.

56. Dharmaraj, N., Viswanathamurti, P., and Natarajan, K. (2001) Ruthenium(II) complexes containing bidentate Schiff bases and their antifungal activity. *Transition Metal Chemistry*, **26**, 105–109.